Elevated NMDA receptor levels and enhanced postsynaptic long-term potentiation induced by prenatal exposure to valproic acid

Tania Rinaldi*, Karina Kulangara†, Katia Antoniello*, and Henry Markram*‡

*Laboratory of Neural Microcircuits and †Laboratory of Cellular Neurobiology, Brain Mind Institute, Ecole Polytechnique Fédérale de Lausanne, CH 1015 Lausanne, Switzerland

Communicated by Kenneth B. Eisenthal, Columbia University, New York, NY, June 11, 2007 (received for review February 7, 2007)

Valproic acid (VPA) is a powerful teratogen causing birth defects in humans, including autism spectrum disorder (ASD), if exposure occurs during the first trimester of embryogenesis. Learning and memory alterations are common symptoms of ASD, but underlying molecular and synaptic alterations remain unknown. We therefore studied plasticity-related mechanisms in the neocortex of 2-week-old rats prenatally exposed to VPA and tested for changes in glutamate-mediated transmission and plasticity in the neocortex. We found a selective overexpression of NR2A and NR2B subunits of NMDA receptors, as well as the commonly linked kinase calcium/calmodulin-dependent protein kinase II. Synaptic plasticity experiments between pairs of pyramidal neurons revealed an augmented postsynaptic form of long-term potentiation. These results indicate that VPA significantly enhances NMDA receptor-mediated transmission and causes increased plasticity in the neocortex. Enhanced plasticity introduces a surprising perspective to the potential molecular and synaptic mechanisms involved in children prenatally exposed to VPA.

autism | *in vitro* electrophysiology | plasticity | somatosensory cortex | NMDA receptors

Autism is a developmental disorder of neurological origin primarily affecting social cognition. Its etiology has not yet been clarified, but genetic and environmental contributions to neurodevelopmental alterations either cause or confer vulnerability to this disorder (1). The teratogens that have been most clearly linked to autism include thalidomide (2) and valproic acid (VPA) (3–7). These drugs can cause diverse birth defects, but over a narrow time window of vulnerability (days 20–24 of human pregnancy), they have a higher likelihood of causing autism (8, 9). The core symptoms of autism, first identified by Leo Kanner in 1943 (10), are centered around inappropriate social interaction, poor or no language development, enhanced sensory sensitivity, repetitive behaviors, attention abnormalities, and resistance to novel environments (11). Most affected children tend to have a lower IQ than their peers, but the extent to which the communication deficit has clouded these assessments is not clear. A fraction of autistic children are considered high functioning, with unusually powerful memory capabilities, and children who do solve the communication handicap are often found to have unusual learning and memory capabilities (12–17). There are currently no potential molecular and synaptic candidates for the learning and memory alterations found in autistic children.

Recent studies are focusing more on animal models of autism, which could provide the only means of rapidly exploring molecular, synaptic, and cellular candidates linked to the disorder. The rat VPA model is one example of an insult-based model that is being increasingly explored (9, 18–21). Offspring of pregnant rats exposed to a single injection of VPA display some of the gross anatomical changes (18, 22) and core behavioral symptoms observed in autism, such as impaired social interactions, increased repetitive behaviors, and a higher level of anxiety (20, 23, 24). A recent study also found exaggerated fear memories in this animal model (24). Although any animal model of autism is unlikely to entirely reflect a human disorder, the fact that the same teratogen that has been linked to autism also triggers a number of alterations similar to those associated with the disorder suggests that this model may be a good starting point for the search for molecular and synaptic candidates involved in autism.

Results

Increased Protein Expression Levels of NMDA Receptor Subunits NR2A and NR2B. We studied the VPA rat model for molecular and synaptic changes related to glutamatergic transmission and altered synaptic plasticity and began by examining the expression levels of some of the key proteins known to be involved in cortical plasticity (25–27). We tested for expression of protein kinases and for the different glutamate receptor subunits by Western blotting on tissue samples of the somatosensory cortex of 2-week-old offspring of control and VPA-treated dams.

We found that the level of calcium/calmodulin-dependent protein kinase II (CaMKII) was significantly increased by >60% (control, $n = 11$, 100 ± 9%; treated, $n = 11$, 169 ± 24%; $P < 0.05$), whereas the expression level of ERK and cAMP response element binding protein (CREB) was not changed in VPA-treated rats (Fig. 1*A*). The expression levels of α-amino-3-hydroxy-5-methyl-4-isoxazolepropionic acid (AMPA) receptor subunits GluR1, GluR2, and GluR3 (Fig. 1*B*) and the obligatory subunit of the NMDA receptor, NR1, were unaltered (Fig. 1*C*). However, the expression level of the NMDA receptor subunits NR2A and NR2B were 2-fold increased (control NR2A, $n = 8$, 100 ± 28%; treated NR2A, $n = 8$, 230 ± 22%; $P < 0.01$; control NR2B, $n = 7$, 100 ± 11%; treated NR2B, $n = 8$, 220 ± 28%; $P < 0.01$; Fig. 1*C*). Because enhanced NMDA receptor levels have been shown to render neurons more vulnerable to neurotoxicity (28), we studied apoptosis, but did not find any increased form of active cell death in the cortex of VPA-treated rats (data not shown). However, such high levels of NMDA receptors may make the neocortex more vulnerable to insult and neurotoxicity as development proceeds. We also measured the expression levels of some phosphorylated forms of these proteins (pCREB-S133, pCaMKII-T286/287, pERK-Thr-202/Tyr-204, pGluR1-S831, pGluR1-S845, pNR1-S896, pNR1-S897, and pNR2B-

Author contributions: T.R. and H.M. designed research; T.R., K.K., and K.A. performed research; K.K. contributed new reagents/analytic tools; T.R. analyzed data; and T.R. and H.M. wrote the paper.

The authors declare no conflict of interest.

Abbreviations: aCSF, artificial cerebral spinal fluid; AMPA, α-amino-3-hydroxy-5-methyl-4-isoxazolepropionic acid; ASD, autism spectrum disorder; LTP, long-term potentiation; VPA, valproic acid.

‡To whom correspondence should be addressed. E-mail: henry.markram@epfl.ch.

This article contains supporting information online at www.pnas.org/cgi/content/full/0704391104/DC1.

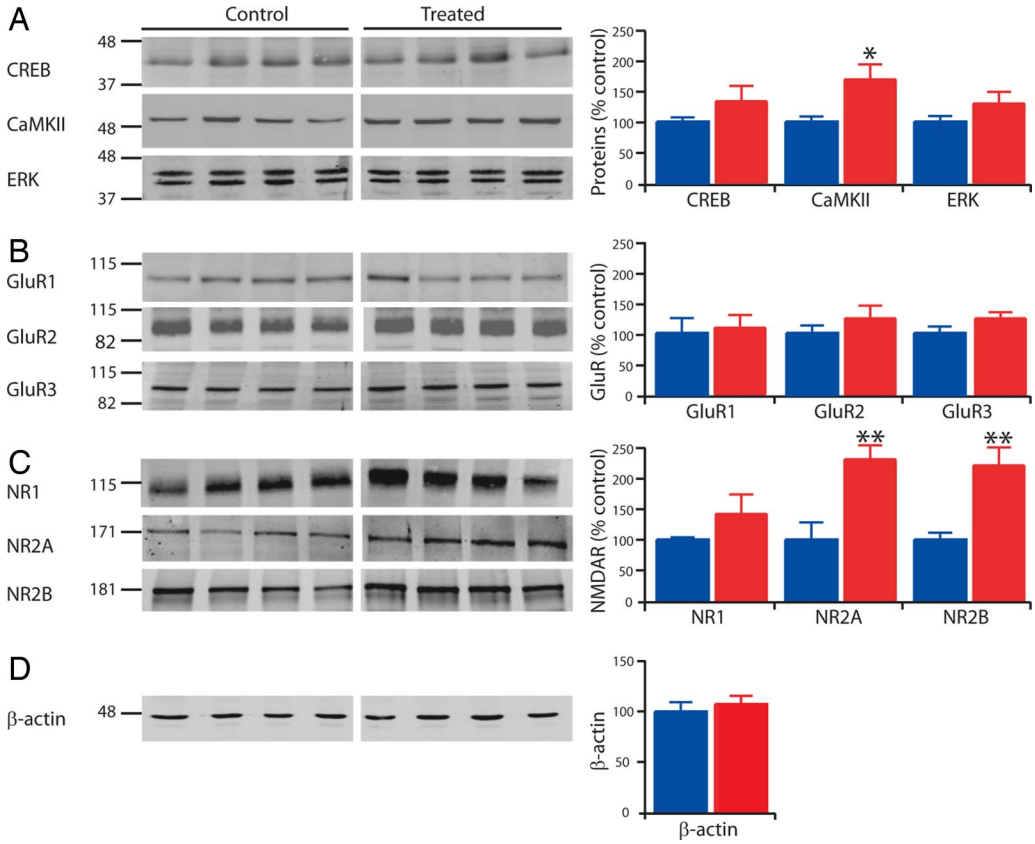

Fig. 1. Enhanced CaMKII, NR2A, and NR2B protein expression levels. Examples of Western blots and mean values reported as percentage of control, normalized to in-lane control (β-actin). (*A*) Western blots of CREB ($n = 6$ and 7), CamKII ($n = 11$ and 11), and ERK ($n = 12$ and 12). (*B*) Western blots of AMPA receptor subunits GluR1 ($n = 8$ and 9), GluR2 ($n = 8$ and 8), and GluR3 ($n = 8$ and 8). (*C*) Western blots of NMDA receptor subunits NR1 ($n = 8$ and 8), NR2A ($n = 8$ and 8), and NR2B ($n = 7$ and 8). (*D*) Western blots of β-actin ($n = 12$ and 12). Data show mean ± SEM. *, $P < 0.05$; **, $P < 0.01$).

S1303), as well as some metabotropic glutamate receptor subunits (mGluR1, mGluR5, mGluR4, and mGluR6/7) and the kainate receptor subunits (GluR6/7), and found no difference between control and VPA-treated rats [supporting information (SI) Table 1]. This result indicates that the elevated NMDA receptor level is a highly selective abnormality within the glutamatergic system.

Increased NMDA Receptor-Mediated Synaptic Currents. To determine whether the enhanced expression of the NR2A and NR2B subunits translated into a functional increase of NMDA receptor-mediated synaptic current, we performed multineuron patch-clamp experiments on slices of the somatosensory cortex. We examined directly the synaptic currents mediated by AMPA and NMDA receptors between pairs of layer 2/3 pyramidal neurons (Fig. 2). We found that the percentage of charge entering the postsynaptic cell through the NMDA receptors, calculated as the ratio of the charge entering the cell when AMPA receptors are blocked and when both AMPA and NMDA receptors are available, was significantly larger in VPA-treated rats (control, $n = 12$, 39 ± 2%; treated, $n = 10$, 69 ± 7%; $P < 0.01$). Similarly, the ratio of the charge entering the cell through the AMPA versus the NMDA receptors was significantly smaller in treated rats (control, $n = 12$, 1.7 ± 0.2; treated, $n = 10$, 0.7 ± 0.2; $P < 0.01$; Fig. 2*C*) because of a greater current influx through the NMDA receptors. The decay time courses of the NMDA receptor-mediated currents were unaffected, suggesting that the kinetics are normal (SI Fig. 5). NR2A- and NR2B-containing receptors express different deactivation kinetics (25). This result suggests there is a similar proportional increase in the insertion of NR2A- and NR2B-containing receptors at these synapses.

Increased Postsynaptic Long-Term Potentiation (LTP). Because both NMDA receptors (25) and CamKII (26) are critically involved in plasticity, learning, and memory, we next examined whether synaptic plasticity was altered after a Hebbian learning in layer 2/3 pyramidal neurons (Fig. 3 *A* and *B*). We found a much larger increase in the amplitude of the synaptic response after pairing in VPA-treated rats (control, $n = 12$, 69 ± 22%; treated, $n = 14$, 207 ± 59%; $P < 0.05$; Fig. 3*C*).

We also observed this alteration in layer 5 pyramidal neurons when we examined plasticity in direct connections (Fig. 3 *D* and *E*), indicating that enhanced potentiation is not unique to layer 2/3. For these neurons, we used a slightly different protocol to understand more precisely what synaptic parameters were altered by the pairing protocol. The test stimulation allowed us, with a model of dynamic synaptic transmission, to extract three parameters of the connection (*A*, the absolute synaptic efficacy; *Pr*, equivalent to the probability of release; *D*, time constant to recover from depression) (29) before and after pairing. *Pr* changed equally in both control and treated rats, which is the typical presynaptic form of synaptic plasticity found in the neocortex at this age (30). The absolute strength, *A*, was hardly changed in control rats, but greatly enhanced in VPA-treated rats (control, $n = 12$, 106 ± 8%; treated, $n = 11$, 133 ± 8%; $P < 0.05$; Fig. 3*E*). An increase in synaptic strength is typically because of postsynaptic mechanisms, such as an increase in the total number and efficacy of postsynaptic receptors and synapses (31, 32). The time constants for synaptic depression were

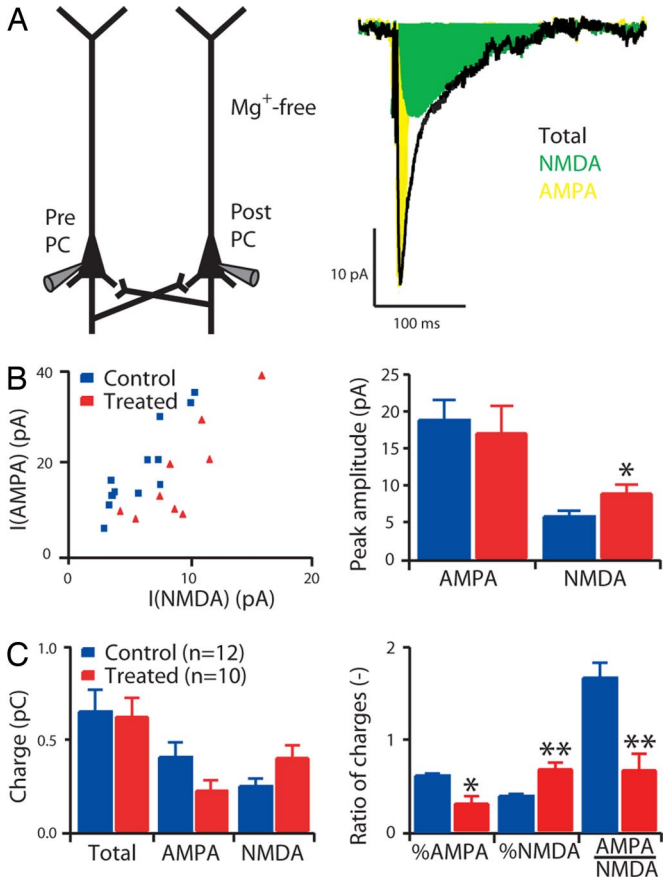

Fig. 2. Enhanced NMDA receptor-mediated synaptic currents. (*A*) Experimental scheme and example of averaged responses (30 sweeps) in the postsynaptic cell before (total) and after blocking of AMPA receptors with NBQX (NMDA). The difference between the control and NMDA traces give the AMPA trace. (*B*) Peak currents of AMPA and NMDA responses. (*C*) Charge entering the postsynaptic cell through AMPA and NMDA receptors (total), NMDA receptors only (NMDA), and AMPA receptors only (AMPA); percentage of charge entering the postsynaptic cell through AMPA receptors and NMDA receptors when no pharmacological blocker is applied (% AMPA and % NMDA, respectively), and ratio between the charge entering the postsynaptic cell through AMPA receptors and the charge entering the postsynaptic cell through the NMDA receptors (AMPA/NMDA). Data show mean ± SEM. *, $P < 0.05$; **, $P < 0.01$.

unaltered in the treated rats. Although the classical coefficient of variation method for quantal analysis of synaptic responses allows unambiguous identification of pre- and postsynaptic loci underlying synaptic plasticity only when extensive simplifying restrictions are made (33), we applied it to our data. The results confirm the higher postsynaptic potentiation component in treated rats (SI Fig. 7).

Normal Action Potential-Evoked Calcium Transient. Enhanced synaptic plasticity may also be due to increased calcium influx through voltage-activated calcium channels (34, 35). Therefore, we examined changes in calcium concentration in these pyramidal neurons in response to back-propagating action potentials (36, 37). We patched a pyramidal neuron, loaded it with a calcium indicator (calcium green-1; see *Materials and Methods*), and observed the change in fluorescence in the dendrites. The protocol involved a single action potential as well as a train of action potentials (Fig. 4*A*). We observed no alteration in the calcium signal at the soma or in the proximal dendrites, both in terms of change in the amplitude (Fig. 4*B*) or in the decay time constant (Fig. 4*C*) of the fluorescent transient, suggesting that calcium influx and handling is normal in the pyramidal neurons of the VPA-treated rats.

Discussion

We examined alterations in the glutamatergic system and related second-messenger pathways in rats prenatally exposed to VPA. We report that a single prenatal injection of VPA causes a surprising and selective overexpression of the NMDA receptor subunits NR2A and NR2B, as well as the closely linked kinase CaMKII. The overexpression of the NMDA receptor subunits translates into enhanced NMDA receptor-mediated synaptic currents and into an amplified postsynaptic form of synaptic plasticity in neocortical pyramidal neurons.

VPA was injected in rats at embryonic day 11.5, at an age when the neural tube closes (9). At this time, neurons are not yet in place in the cortex. The results presented in this study can therefore only be indirect consequences of the initial injury caused by the drug treatment. There is no clear explanation yet of how this treatment alters cortical function.

Selective Alteration Within the Glutamatergic System. The glutamatergic system includes a number of different iono- and metabotropic receptors. We found no alterations in the expression of metabotropic receptors. Of the ionotropic receptors, AMPA and kainate receptors, which mediate most of the fast glutamatergic current, were also unaffected. The selective overexpression of NMDA receptors, which is the key receptor underlying synaptic plasticity in the neocortex, suggests that an important aspect of the alterations in rats exposed to VPA is related to synaptic plasticity.

There are multiple subunits involved in the formation of NMDA receptors. The overexpression of NMDA receptors was not associated with an overexpression of NR1, the obligatory subunit of NMDA receptors. However, it has been shown that this subunit is normally highly expressed, allowing a considerable dynamic range in the expression of functional NMDA receptors. The selectivity of the alteration within the glutamatergic system further extended into the NMDA receptor subunits, in that only the NR2A and NR2B subunits were overexpressed. NMDA receptors can also be formed by NR2C, NR2D, and NR3A, but these subunits are mainly expressed in brain regions other than in the neocortex (25, 38, 39), and were therefore not studied here.

Indications of Unaltered NMDA Receptor Subunits' Development. NMDA receptors containing NR2A or NR2B subunits generate high-channel conductance openings with a high sensitivity to the voltage-dependent block by Mg^{2+} (40). These NMDA receptor subunits are known to be differentially expressed during development, with the expression of NR2B already high at birth and throughout postnatal development before declining during adulthood. However, NR2A expression appears around P7 and increases during the next 2 or 3 weeks to adult levels (25). We found a similar increase in both NR2A and NR2B subunits (i.e., the same ratio of the expression level of these two proteins between control and treated rats and no change in time course of the NMDA receptor-mediated synaptic currents). Although we do not have direct proof that this result is not due to a failure of the synapse to mature, the similar increase in both subunits suggests that VPA-treatment does not affect these developmental changes in the brain.

Selective Postsynaptic Plasticity Enhancement. The second messenger most closely linked to NMDA receptors, CaMKII, was also overexpressed in the VPA-treated rats. CamKII is a critical messenger mediating synaptic plasticity, experience-dependent synaptic changes, and memory (26, 41–43). Indeed, we found enhanced LTP in the VPA-treated rats. LTP in the neocortex at

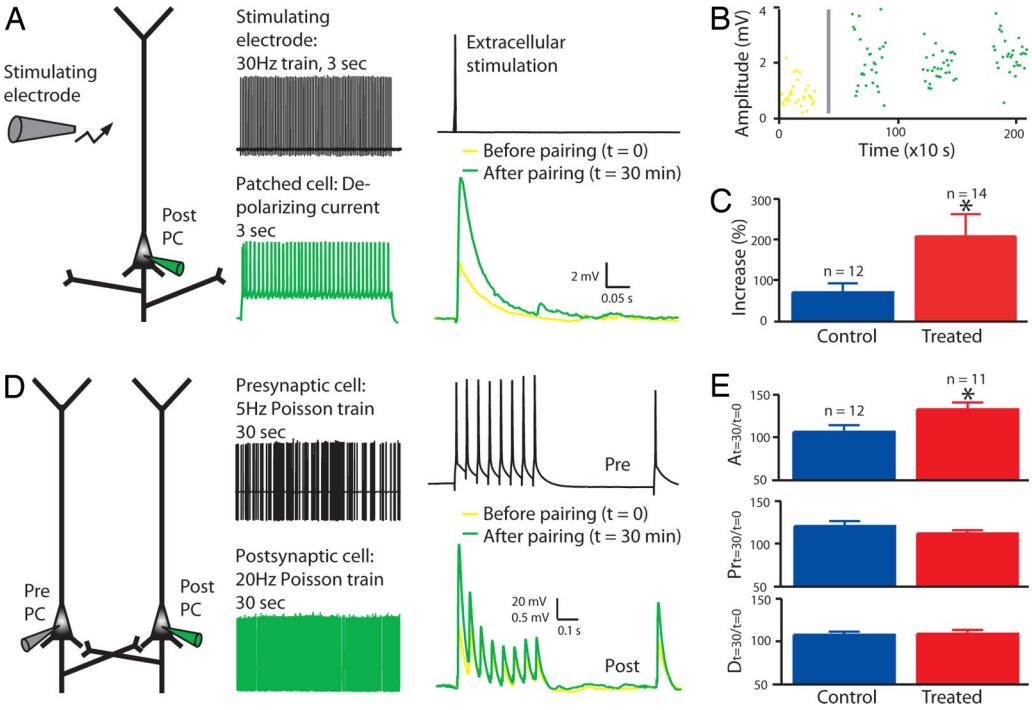

Fig. 3. Enhanced postsynaptic plasticity. (*A–C*). LTP with extracellular stimulation in layer 2/3 pyramidal neurons. (*A*) Experimental scheme, pairing protocol, and example of mean response in a patched cell, before and after pairing. (*B*) Example of response amplitude as a function of time. The gray line represents the timing of the pairing protocol. (*C*) Mean of percentage increase in the amplitude of the response to extracellular stimulation after pairing. The absolute values of the response amplitudes are displayed in SI Fig. 6. (*D* and *E*) LTP in direct connections between layer 5 pyramidal neurons. (*D*) Experimental scheme, pairing protocol, and example of mean responses in the postsynaptic cell before and after pairing. (*E*) Mean of percentage change after pairing of the absolute synaptic efficacy *A*, the probability of release *Pr*, and the time constant for depression *D*. The absolute values of *A*, *Pr*, and *D* before and after pairing are displayed in SI Fig. 6. Data show mean ± SEM. *, $P < 0.05$.

this age is more typically a presynaptic form (29, 30), and we found that, although the presynaptic LTP remained intact, the postsynaptic LTP was significantly enhanced. CaMKII has been shown to be a key messenger mediating the postsynaptic form of LTP by enhancing the insertion of AMPA receptors into the postsynaptic density (44). It has also been shown that NMDA receptors can control synaptic plasticity by regulating postsynaptic AMPA receptors (25). It could therefore be that maximal

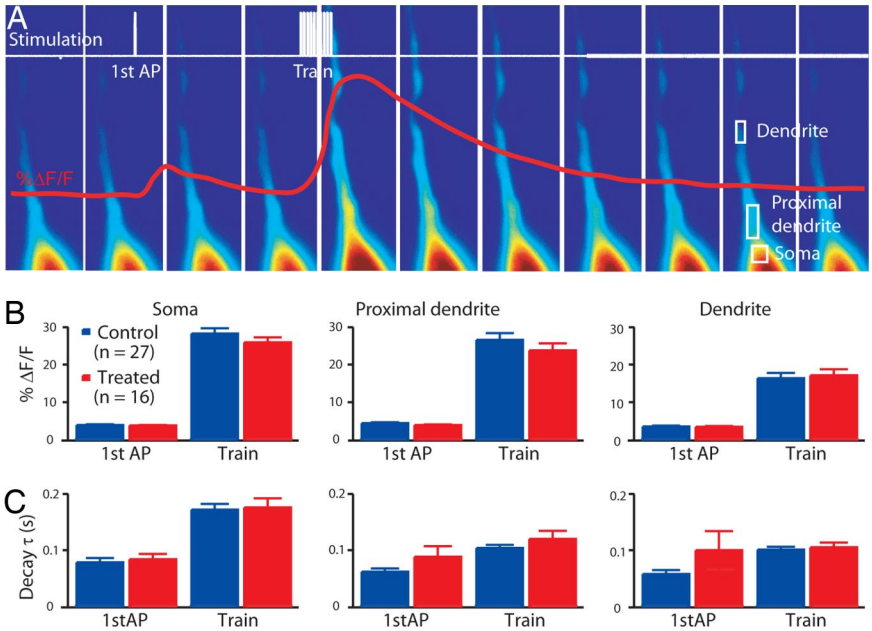

Fig. 4. Unchanged calcium transient. (*A*) Scheme of stimulation protocol and example of fluorescence in a patched pyramidal neuron. (*B*) Percentage of change in the calcium signal in the first action potential and train stimulation at the three locations of analysis (at the soma, at the proximal apical dendrite, and on the dendrite, 50 μm away from the soma). (*C*) Decay time constant of the calcium signal at the corresponding locations. Data show mean ± SEM.

presynaptic changes were already induced in the control rats and that additional NMDA receptors and CaMKII expression could not enhance this form of LTP further.

In summary, we report that a single prenatal injection of VPA causes a surprisingly selective enhancement of protein expression of the NMDA receptor subunits NR2A and NR2B, as well as the closely linked kinase CaMKII. These changes translate into enhanced NMDA receptor-mediated synaptic currents and a greatly amplified postsynaptic form of synaptic plasticity in neocortical pyramidal neurons. These results suggest molecular and synaptic alterations in children prenatally exposed to VPA. It is known that many of these children suffer from what is known as fetal anticonvulsant syndrome, and as many as 60% suffer from two or more of the core symptoms of autism (4). Further investigations are required to determine whether NMDA receptors are up-regulated in these cases.

Materials and Methods

The VPA Rat Model of Autism. All experimental procedures were carried out according to the Swiss Federation rules for animal experiments. Wistar Han rats (Charles River Laboratories, L'Arbresle, France) were mated, with pregnancy determined by the presence of a vaginal plug on embryonic day 0. The sodium salt of VPA (NaVPA; Sigma–Aldrich, St. Louis, MO) was dissolved in 0.9% saline for a concentration of 150 mg/ml (pH 7.3). The dosing volume was 3.3 ml/kg, and the dosage was adjusted according to the body weight of the dam on the day of injection. Treated rats received a single i.p. injection of 500 mg/kg NaVPA on gestational day 11.5, and control rats were untreated (18). We verified that saline-injected rats did not show any difference in behavior compared with control (data not shown). Unchanged litter size, pup body weight, and general health of the mothers and pups (data not shown) were indications of normal rearing conditions for treated rats.

Dams were housed individually and allowed to raise their own litters. The offspring were used for experiments on postnatal days 12–16.

Western Blotting. Samples from rat brain were dissected, and the entire brains were frozen in isopentane (−50°C) within 45 sec and then stored at −80°C. Tissue punches of the primary somatosensory cortex were extracted and homogenized in sucrose buffer (0.32 M sucrose, 10 mM Hepes, protease inhibitors 0.3 mM PMSF, 0.7 μg/ml Pepstatin, 2 μg/ml Aprotinin, 2 μg/ml Leupeptin) by using a homogenizer (Eurostar Digital 248200; IKA-Werke, Staufen, Germany). Triton was added to a final concentration of 1%. For the study of the proteins CREB, pCREB, mGluR1, mGluR5, mGluR4, and mGluR6/7, tissue punches were sonicated in 1% SDS. Protein concentration was determined by using the Bio-Rad (Hercules, CA) protein assay, and Lämmli 2× was added. Then 15 μg of each sample was separated by SDS/PAGE, and proteins were transferred onto Protran BA83 nitrocellulose membrane (Schleicher & Schuell, Riehen, Switzerland) and blocked in Odyssey (Li-Cor Biosciences, Lincoln, NE) diluted in PBS according to the manufacturer's protocol. The membranes were probed with the indicated antibodies. The antibodies against the following proteins were applied for Western blotting: monoclonal antibodies anti-CamKII 1:10,000 (Upstate Biotechnology, Lake Placid, NY), anti-GluR2 1:200 (BD Biosciences, San Jose, CA), anti-GluR3 1:500 (Zymed Laboratories, South San Francisco, CA), anti-NR2B 1:250 (BD Biosciences), anti-pCREB S133 1:1,000 (Upstate Biotechnology), and anti-β-actin 1:2,000 (Chemicon International, Temecula, CA); polyclonal antibodies anti-CREB 1:1,000 (Upstate Biotechnology), anti-ERK 1:1,000 (Cell Signaling Technology, Danvers, MA), anti-pERK Thr-202/Tyr-204 1:1,000 (Upstate Biotechnology), anti-pCamKII T286/287 1:1,000 (Upstate Biotechnology), anti-GluR1 1:300 (Chemicon International), anti-pGluR1 S831 1:500 (Upstate Biotechnology), anti-pGluR1 S845 1:500 (Upstate), anti-NR1 1:500 (Upstate Biotechnology), anti-pNR1 S896 1:500 (Upstate), anti-pNR1 S897 1:250 (Upstate Biotechnology), anti-NR2A 1:250 (Upstate Biotechnology), anti-pNR2B S1303 1:500 (Upstate Biotechnology), anti-mGluR1 1:250 (Upstate Biotechnology), anti-mGluR5 1:1,000 (Upstate Biotechnology), anti-mGluR4 1:1,000 (Abcam, Cambridge, MA), anti-mGluR67 1:1,000 (Abcam), and anti-GluR6/7 1:200 (Upstate Biotechnology); and secondary Alexa Fluor800-coupled goat anti-rabbit IgG and secondary Alexa Fluor800- or 700-coupled goat anti-mouse IgG (W: 1:2,000; Molecular Probes, Eugene, OR). The fluorescence intensity of the infrared dye-labeled secondary antibodies bound to the primary antibodies was quantified by using the integrated Odyssey software. The ratio of the signal from the different proteins to β-actin protein was used to normalize the signal intensities and correct for loading and sampling errors. All data are reported as percentage of control. Phosphoproteins are reported as the ratio of phosphorylated over total protein levels.

Acute Slice Preparation. Offspring (postnatal days 12–16) were rapidly decapitated and sagittal neocortical slices (300 μm thick) were sectioned on a vibratome (HR2; Sigmann Elektronik, Hüffenhardt, Germany) in iced artificial cerebral spinal fluid (aCSF). Optimal slices, with apical dendrites of cells running parallel to the slice surface, were selected for recording. They were incubated for 30 min at 35°C and then at room temperature until transferred to the recording chamber (34°C). The aCSF contained 125 mM NaCl, 2.5 mM KCl, 25 mM glucose, 25 mM $NaHCO_3$, 1.25 mM NaH_2PO_4, 2 mM $CaCl_2$, and 1 mM $MgCl_2$. For the LTP experiment with extracellular stimulation, the aCSF also contained 10 μM bicuculline.

For the study of NMDA receptor-mediated synaptic currents, the aCSF was prepared without $MgCl_2$ and contained 10 μM NBQX for the isolation of the NMDA component. Neurons in somatosensory cortex were identified by using IR-DIC microscopy with an upright microscope [Olympus (Tokyo, Japan) BX51WI, fitted with a ×60/0.90-W objective]. Recorded neurons were selected up to 70 μm below the surface of the slice.

Electrophysiological Recording. Simultaneous whole-cell recordings from clusters of up to four neurons (pipette resistance 4–10 MΩ) were made, and signals were amplified by using Axopatch 200B amplifiers (Axon Instruments, Union City, CA). Voltages (in current-clamp mode) or current (in voltage-clamp mode) were recorded with pipettes containing 100 nM potassium gluconate, 20 mM KCl, 4 mM ATP-Mg, 10 mM phosphocreatine, 0.3 mM GTP, 10 mM Hepes and 0.5% biocytin (pH 7.3, 270–300 mOsm). Membrane potentials were not corrected for the junction potentials between pipette and bath solution (≈10 mV).

NMDA-Mediated Synaptic Currents. Direct synaptic connections were examined between voltage-clamped layer 2/3 pyramidal neurons by eliciting a single-pulse stimulation in the presynaptic cell. (The results of these experiments would not have been as accurate in layer 5 pyramidal neurons because these cells are too big to be voltage-clamped in a satisfactory manner because of well known space-clamp limitations). The amplitude, decay time constant, and integral (i.e., the charge) of the average response (average of 30 traces) in the postsynaptic cell in the absence (total) and presence (NMDA) of 10 μM NBQX in the aCSF were measured. The AMPA response was calculated as the difference between the total and NMDA responses. The total number of connections studied was 12 for control and 10 for VPA-treated rats.

LTP with Extracellular Stimulation. An extracellular electrode was placed 100 to 300 μm away from the whole-cell-patched layer 2/3 pyramidal neurons. An electrical stimulus that produced a postsynaptic response in the recorded neurons of 2–4 mV in amplitude was given before the pairing protocol. Responses to 30 such stimuli delivered at a rate of 0.1/sec were recorded and averaged. The 3-sec-long pairing protocol consisted of a 30-Hz regular train stimulation to the extracellular electrode simultaneously with a depolarization above the threshold of the patched cell, applied twice with 30-sec intervals. After pairing, three further data sets, each consisting of responses to 30 stimuli delivered at 0.1/sec were collected with 5-min pauses separating these stimulus trains. The percent increase in the amplitude of response to the stimulation pulse after pairing compared with before pairing was measured. The total number of pyramidal neurons studied was 13 for control and 14 for VPA-treated rats.

LTP in Direct Connections. Direct synaptic connections were examined between whole-cell-patched thick-tufted layer 5 pyramidal neurons by eliciting short trains (eight pulses) of precisely timed action potentials at 30-Hz frequency, followed by a recovery test response 500 msec later. The average synaptic response (average of 30 traces) to this stimulation protocol allows the extraction of the basic parameters of the synaptic connection with a model of dynamic synaptic transmission (*A*, absolute strength of the connection; *Pr*, equivalent to the probability of release; *D*, time constant to recover from depression) (29). The pairing protocol, applied twice 5 and 10 min after the initial test protocol, consisted of a 30-sec-long Poisson train stimulation of 5- and 20-Hz frequency to the pre- and postsynaptic cells, respectively. Excitatory postsynaptic potentials were then recorded for a further 30 min at 0.1 spikes per sec. The total number of connections studied was 12 for control and 11 for VPA-treated rats.

Calcium Imaging. Calcium green-1 diluted in the intracellular solution (500 μM; Molecular Probes; 488 nm excitation; 515–560 nm emission) was loaded into patched neurons, and fluorescence was recorded by a CCD camera (Imago CCD; TILL Photonics, Gräfelfing, Germany) controlled by a computer. The stimuli to the patched thick-tufted layer 5 pyramidal neurons consisted of an action potential, followed by a train of action potentials 1 sec later; it was applied after 1 sec of basal fluorescent recording. Images were taken at 7-Hz sampling frequency (50 msec exposure time) and measured and analyzed with TILLVision Softare version 4.00 (TILL Photonics Imaging System Software, Gräfelfing, Germany). Fluorescent recordings were normalized to the basal fluorescence ($\% \ \Delta F = (F - F_{\text{basal}})/F_{\text{basal}} \times 100$). Single exponentials were fitted from the peak of ΔF to the basal value to extract the decay time constant of the signal (decay τ). The measures were done in three regions of interest: at the soma, at the proximal dendrite, and at the apical dendrite 50 μm away from the soma. The total number of cells studied was 27 for control and 16 for treated rats.

Statistical Analysis. For comparison of means, we used Student's *t* tests. Statistics reported in the text and figures represent the mean ± SEM.

We thank Gilad Silberberg, Phil Goodman, Brandi Mattson, Michele Pignatelli, Thomas Berger, Jean-Vincent Le Bé, and Sonia Garcia for their help. This work was supported by the National Alliance for Autism Research and by a grant from the European Commission for the EUSynapse project.

1. Persico AM, Bourgeron T (2006) *Trends Neurosci* 29:349–358.
2. Stromland K, Nordin V, Miller M, Akerstrom B, Gillberg C (1994) *Dev Med Child Neurol* 36:351–356.
3. Christianson AL, Chesler N, Kromberg JG (1994) *Dev Med Child Neurol* 36:361–369.
4. Moore SJ, Turnpenny P, Quinn A, Glover S, Lloyd DJ, Montgomery T, Dean JC (2000) *J Med Genet* 37:489–497.
5. Rasalam AD, Hailey H, Williams JH, Moore SJ, Turnpenny PD, Lloyd DJ, Dean JC (2005) *Dev Med Child Neurol* 47:551–555.
6. Williams G, King J, Cunningham M, Stephan M, Kerr B, Hersh JH (2001) *Dev Med Child Neurol* 43:202–206.
7. Williams PG, Hersh JH (1997) *Dev Med Child Neurol* 39:632–634.
8. Arndt TL, Stodgell CJ, Rodier PM (2005) *Int J Dev Neurosci* 23:189–199.
9. Rodier PM, Ingram JL, Tisdale B, Croog VJ (1997) *Reprod Toxicol* 11:417–422.
10. Kanner L, Eisenberg L (1957) *Psychiatr Res Rep Am Psychiatr Assoc* April(7):55–65.
11. Rapin I, Katzman R (1998) *Ann Neurol* 43:7–14.
12. Bennetto L, Pennington BF, Rogers SJ (1996) *Child Dev* 67:1816–1835.
13. Frith U (2004) *J Child Psychol Psychiatry* 45:672–686.
14. Minshew NJ, Goldstein G (2001) *J Child Psychol Psychiatry* 42:1095–1101.
15. Mottron L, Belleville S, Stip E, Morasse K (1998) *Memory* 6:593–607.
16. Mottron L, Morasse K, Belleville S (2001) *J Child Psychol Psychiatry* 42:253–260.
17. O'Shea AG, Fein DA, Cillessen AH, Klin A, Schultz RT (2005) *Dev Neuropsychol* 27:337–360.
18. Ingram JL, Peckham SM, Tisdale B, Rodier PM (2000) *Neurotoxicol Teratol* 22:319–324.
19. Miyazaki K, Narita N, Narita M (2005) *Int J Dev Neurosci* 23:287–297.
20. Schneider T, Przewlocki R (2005) *Neuropsychopharmacology* 30:80–89.
21. Stanton ME, Peloso E, Brown KL, Rodier P (2007) *Behav Brain Res* 176:133–140.
22. Rodier PM, Ingram JL, Tisdale B, Nelson S, Romano J (1996) *J Comp Neurol* 370:247–261.
23. Schneider T, Labuz D, Przewlocki R (2001) *Pol J Pharmacol* 53:531–534.
24. Markram K, Rinaldi T, Mendola DL, Sandi C, Markram H (2007) *Neuropsychopharmacology*, in press.
25. Kim MJ, Dunah AW, Wang YT, Sheng M (2005) *Neuron* 46:745–760.
26. Lisman J, Schulman H, Cline H (2002) *Nat Rev Neurosci* 3:175–190.
27. Mammen AL, Kameyama K, Roche KW, Huganir RL (1997) *J Biol Chem* 272:32528–32533.
28. McDonald JW, Johnston MV (1993) *NIDA Res Monogr* 133:185–205.
29. Tsodyks MV, Markram H (1997) *Proc Natl Acad Sci USA* 94:719–723.
30. Markram H, Tsodyks M (1996) *Nature* 382:807–810.
31. Markram H, Tsodyks M (1996) *J Physiol Paris* 90:229–232.
32. Selig DK, Nicoll RA, Malenka RC (1999) *J Neurosci* 19:1236–1246.
33. Faber DS, Korn H (1991) *Biophys J* 60:1288–1294.
34. Weiss JL, Burgoyne RD (2002) *Trends Neurosci* 25:489–491.
35. Burgess DL, Noebels JL (1999) *Ann NY Acad Sci* 868:199–212.
36. Markram H, Helm PJ, Sakmann B (1995) *J Physiol* 485:1–20.
37. Spruston N, Schiller Y, Stuart G, Sakmann B (1995) *Science* 268:297–300.
38. Wenzel A, Fritschy JM, Mohler H, Benke D (1997) *J Neurochem* 68:469–478.
39. Takai H, Katayama K, Uetsuka K, Nakayama H, Doi K (2003) *Exp Mol Pathol* 75:89–94.
40. Cull-Candy S, Brickley S, Farrant M (2001) *Curr Opin Neurobiol* 11:327–335.
41. Otmakhov N, Griffith LC, Lisman JE (1997) *J Neurosci* 17:5357–5365.
42. Giese KP, Fedorov NB, Filipkowski RK, Silva AJ (1998) *Science* 279:870–873.
43. Silva AJ, Stevens CF, Tonegawa S, Wang Y (1992) *Science* 257:201–206.
44. Liao D, Hessler NA, Malinow R (1995) *Nature* 375:400–404.